AJP

ISSN : 0971 - 3093

Vol 28, Nos 10-12, October-December 2019

ASIAN JOURNAL OF PHYSICS

An International Peer Reviewed Research Journal

Advisory Editors : W. Kiefer & FTS Yu

A Special Issue

Dedicated to

Prof Kehar Singh

Formerly Professor of Physics

at IIT Delhi

Guest Editor : R. S. Sirohi

ap

ANITA PUBLICATIONS

FF-43, 1st Floor, Mangal Bazar, Laxmi Nagar, Delhi-110 092, India

B O : 2, Pasha Court, Williamsville, New York-14221-1776, USA

ap

Asian Journal of Physics
Vol. 28, Nos 10-12 (2019) 777-786
Available on: www.asianjournalofphysics.in

Transport of intensity equation for phase imaging: A review

Alok K Gupta and Naveen K Nishchal
Department of Physics, Indian Institute of Technology Patna,
Bihta, Patna-801 106, India

This article is dedicated to Prof Kehar Singh for his significant contributions to Optics and Photonics

Quantitative phase imaging has attracted widespread attention of the research community because of its extensive applications in metrology and biological sciences. The techniques are broadly divided into interferometric and non-interferometric categories. The transport of intensity equation (TIE) based phase imaging method comes under the non-interferometric category. The TIE has usual advantages over the interferometric techniques because of partial coherence illumination and direct phase recovery without any unwrapping complexity. However, it has some limitations also such as paraxial approximation, near Fresnel region diffraction, and knowledge of appropriate boundary conditions. This article reviews the difficulties and complexities while solving the TIE for accurate quantitative phase map.

Keywords: Non-interferometric phase imaging, Transport of intensity equation, Quantitative phase imaging

1 Introduction

The pure phase objects are those samples which are having thickness unevenness or refractive index variation and are mostly transparent to the illuminating light intensity. The micro pure phase samples are difficult to image with conventional imaging modalities. These phase samples do deviate the phase of the light wave. By measuring the phase difference, one can predict the surface morphology up to the nano-level depth. In the recent years, a great interest among scientific community has been developed in quantitative phase imaging (QPI).The QPI has emerged as an important tool for phase visualization and morphological structure analysis. These methods have been very effective especially for non-absorbing specimens such as micro-optical elements and unstained biological cells. Zernike's phase contrast [1] and differential interference contrast microscopy [2] techniques have been proven to be very useful imaging tools for visualization of phase samples. Generally, the phase image obtained with these conventional methods is having the qualitative descriptions in terms of optical path-length measurement. The information is not quantitative as needed for morphological information. However, the phase contrast methods can be further studied for quantitative imaging also with some additional modifications. The method is complex and again an interferometric technique. In a related study [3], spiral phase filter based phase contrast microscopy has been extended for quantitative imaging. It has been demonstrated that a sequence of at least 3 spatially filtered images are needed to record with different rotational orientations of the spiral phase plate to obtain a quantitative reconstruction of both amplitude and phase information of a complex microscopic sample.

The current techniques for QPI can be divided into two main categories. First, the digital holography [4,5], which is interference based method. Digital holographic microscopy (DHM) has been successfully demonstrated in various applications such as optical metrology, biological imaging, and bio-medical applications [6-9]. However, these methods typically rely on interference of light beams with a high degree

Corresponding author :
e-mail: nkn@iitp.ac.in (Naveen K Nishchal)

of coherence. Therefore, the DHM involves many problems such as phase unwrapping and speckle that prevent accurate phase retrieval and formation of high quality images.

The second category is the non-interferometric methods, such as ptychography [10-12] and the transport of intensity equation (TIE) [13-15]. The ptychography is based on intensity distributions which uses iterative phase retrieval techniques to obtain the phase image of the sample. The technique is relatively new and major works are yet to be accomplished to improve the algorithms. The TIE-based approach is a simpler method based on Fresnel propagation which is a non-interferometric and non-iterative technique. The TIE was originally derived by Teague [13] from the Helmholtz equation under paraxial approximation [14]. The TIE has analytical relationship with the object-plane phase and the first derivative of intensity with respect to the optical axis in the near Fresnel region. It allows direct recovery of phase information by just solving a second order differential equation. It was mainly applied in conventional fields such as adaptive optics [16], transmission electron microscopy (TEM) [17,18], material studies [19], X-ray imaging [20], matter wave field [21], and neutron radiography [22]. Recently, it has been brought in the forefront of three-dimensional (3D) depth imaging [23,24] and quantitative phase microscopy [25].

The TIE-based quantitative imaging systems are free from the vibration isolation and phase unwrapping problem. The perfect coherence of illumination source is also not needed for TIE. In the conventional TIE experimental setup, a CCD is mounted on a translation stage. The translation is precisely controlled along the propagation axis and thus multiple defocused images are recorded. There are some drawbacks also in the TIE method such as accuracy and misalignment occurred during translation. Recording of two intensity images is the basic requirement for the TIE computation. For this, either the camera or the object needs to be displaced. This mechanical translation should be precisely controlled and accurately measured. To avoid the displacement issue, several methods have been proposed such as volume holography, chromatic aberration, and with no hardware modification. Our technique uses the chromatic aberration that is inherent to every lens-based imaging system as a phase contrast mechanism. This leads to a simple and inexpensive way of achieving single-shot quantitative phase recovery by a modified Transport of Intensity Equation (TIE) employing spatial light modulators (SLM) and electrically tunable lenses [26-31]. Though these methods help overcoming the displacement issue but still involve problems such as variation in magnification and image alignment. A TIE like equation has been derived in which intensity distributions at different refractive index can be related with phase variation at image plane [32-35].

The mandatory requirement of multiple images makes TIE method less suitable for dynamic imaging applications, therefore single-shot TIE methods have been reported [36-42]. Paganin *et al* used the Beer's law approximation [36] and Zuo *et al* exploited SLM as electrical tuneable lens with tilted mirrors to solve the TIE from single-shot [38]. Zhou *et al* reported a method based on in-line digital holography, in which the defocused intensity images have been reconstructed from a single hologram [41]. In a recent study, a refractive index variation-based single shot TIE set-up has been demonstrated with a liquid crystal variable retarder (LCVR), which is cost effective and efficient [42].

In this paper, the TIE-based non-interferometric method for quantitative phase retrieval is reviewed. In the subsequent sections the generalized version of TIE solution, different methods for intensity derivative estimation, refractive index variation-based TIE, and phase discrepancy due to Teague's assumption estimation have been discussed.

2 Theoretical background

2.1 Phase imaging by TIE

The well-known TIE equation is given by [13,14],

$$\nabla_{\perp} \cdot [I_z(x,y)\, \nabla_{\perp}\phi_z(x,y)] = -\frac{2\pi}{\lambda}\frac{\partial I}{\partial z} \tag{1}$$

where λ is the wavelength of light source and $I_z(x,y)$ and $\phi_z(x,y)$ denote the intensity and phase distributions at a particular plane on the optical axis z, respectively. $\nabla_\perp$ denotes the gradient operator in transverse plane. The phase can be determined from differentiation of intensities at several planes in the near field region. The equation can be simplified as two-dimensional (2D) Poisson equation for solving the phase term. For relating directly to phase distributions, Eq (1) can be expanded as,

$$\begin{aligned} -\frac{2\pi}{\lambda}\frac{\partial I}{\partial z} &= \nabla_\perp I_z(x,y)\nabla_\perp \phi_z(x,y,0) + I_z(x,y)\nabla_\perp^2 \phi_z(x,y,0) \\ &\approx I_0 \nabla_\perp^2 \phi_z(x,y,0) \end{aligned} \tag{2}$$

It is assumed that the intensity is nearly constant (and equal to I_0) such that the first term on the right hand side is small compared to the second term. Rewriting the phase distribution at this plane as $\phi_0(x,y)$, Eq (2) can be simplified as,

$$\nabla_\perp^2 \phi_0(x,y) = -\frac{2\pi}{\lambda I_0}\frac{\partial I_0(x,y)}{\partial z} \tag{3}$$

Equation (3) is the 2D Poisson equation, and can be easily solved by applying 2D fast Fourier transform (FFT) algorithm. Taking Fourier transform of both sides,

$$-4\pi^2(k_x^2 + k_y^2)\Phi_0(k_x,k_y) = -\frac{2\pi}{\lambda I_0}\Im\left[\frac{\partial I_0(x,y)}{\partial z}\right] \tag{4}$$

where Φ_0 denotes the Fourier transform of ϕ_0, k_x and k_y denote the spatial frequencies corresponding to the x and y axes, respectively. $\Im$ denotes the Fourier transform operation. For solving the equation, the expression is inverse Fourier transformed:

$$\phi_0(x,y) = \frac{2\pi}{\lambda I_0}\Im^{-1}\left[\frac{1}{4\pi^2(k_x^2 + k_y^2)}\Im\left[\frac{\partial I_0(x,y)}{\partial z}\right]\right], \tag{5}$$

where $\Im^{-1}$ represents the inverse Fourier transform operation. The intensity derivative dI/dz in Eq (3) can be approximated by the finite difference method using the two defocused intensities at positions Δz and $-\Delta z$,

$$\frac{\partial I_0}{\partial z} \approx \frac{I_{\Delta z}(x,y) - I_{-\Delta z}(x,y)}{2\Delta z} \tag{6}$$

Using Eqs (5) and (6), the phase distributions can be obtained directly with two defocused intensity distributions. The defocused image stacks are captured by translating the CCD camera along the optic axis.

2.2 Generalized solution of TIE

As mentioned above, the TIE is a second order partial differential equation relating the phase function and the intensity distribution. In the section 2.1, the TIE equation has been solved by assuming the intensity to be uniform, thus taken to be constant. For generalized solution of TIE, two Poisson equations would be solved to obtain actual phase map. It is usually solved under the Teague's assumption such that $I\nabla\phi$ in Eq (1) is conservative and can be characterized by an auxiliary function ψ, as

$$\nabla\psi = I\nabla\phi \tag{7}$$

Thus, the TIE can be rewritten as following two Poisson's equations:

$$\nabla_\perp^2 \psi(x,y) = -\frac{2\pi}{\lambda I_0}\frac{\partial I_0(x,y)}{\partial z} \tag{8}$$

and

$$\nabla^2\varphi = \nabla(I^{-1}\nabla\psi) \tag{9}$$

These Poisson equations can be solved using any solver such as the Green's function method, the multi-grid solver, the Zernike polynomial expansion method, the Fourier transform and the cosine transform [43-49].

Though the solution of TIE seems simple, its implementation is difficult because of the associated boundary conditions (BC) [50,51]. The typical boundary conditions are: Dirichlet BC, Neumann BC, and periodic BC. Researchers have solved the TIE directly also without using the BCs. Gureyev and Nugent [46] suggested a way to bypass the difficulty of obtaining appropriate BCs by considering that the intensity vanishes at the boundary. Volkov *et al* [48] proposed another way without any requirement of test object or any experimental conditions by suggesting a mathematical way to nullify the energy slow across the boundary using symmetrisation of input intensity distributions.

2.3 Intensity derivative estimation in TIE

For solving the TIE it is needed to know the in-focused intensity I_0 and axial intensity derivative $\partial I/\partial z$. The in-focus intensity can be easily recorded by the CCD camera on image plane. However, the intensity derivative along the propagation axis cannot be easily obtained. It is conventionally estimated by the finite difference (FD) method, which uses the two out-of-focus images, recorded about the image plane with $\pm\Delta z$ defocus distances [12].

$$\frac{\partial I}{\partial z} \approx \frac{I_{\Delta z}(x,y) - I_{-\Delta z}(x,y)}{2\Delta z} \tag{10}$$

The FD-based approximation, as shown in Eq (10), is valid under the limitation of small defocus distance if the data are noise free. If there is noise and quantization error in the experimental data, the derivative estimation would be unstable [52]. Increasing the defocusing distance provides better signal-to-noise ratio in the derivative estimation. However, it leads to the breakdown in the linear approximation and induces nonlinearity error and loss of high frequency details. Thus, there is a trade-off where Δz has been chosen to maintain balance between the nonlinearity error and the noise effect. The optimal defocusing is dependent on the maximum frequency of the object, as well as the noise level [53,54]. There have been many efforts to overcome this trade-off [55-57]. Waller *et al* extended the TIE beyond the small defocus limit by considering higher order derivatives, which allow improved noise performances by correcting the nonlinearities [56]. In a recent work, Medhi *et al* used a third order polynomial in z and showed that the retrieved phase rides on a characteristically low frequency pedestal. Also, it removes the bias term due to the sharp discontinuities of refractive index [58]. To improve the intensity derivative estimation by using the multiple defocused intensity distributions has been reported [57]. The longitudinal intensity derivative can be estimated as,

$$\frac{\partial I}{\partial z} \approx \sum_{i=-n}^{n} \frac{a_i I_{i\Delta z}(r)}{\Delta z} \tag{11}$$

It offers a kind of flexibility in improving the accuracy and noise reduction in derivative estimation. Several FD estimation methods have been proposed, such as high order FD [53-55], noise reduction FD [56], and least square fitting method [55]. Different techniques for TIE solution, boundary conditions and axial derivative have been compared in the Table 1.

Table 1. Comparison of TIE techniques

Problems	Methods	Pros	Cons
Poisson solvers	Green's function	Simple theory	Extensive computation
	Multi-Grid Zernike polynomials	Simple and fast	Low frequency artefacts
	FFT	Fast and Easy	Periodic BCs
	DCT	Fast	Rectangular aperture required
	Iterative DCT	Arbitrary apertures	Required several iterations

Required boundary conditions (BC)	Homogeneous Dirichlet/ Neumann	Easy	Boundary phase artefact
	Periodic	Implementable by FFT solver	Periodic phase at boundary
	Inhomogeneous Dirichlet/ Neumann	Hard aperture	Boundary phase
Axial derivative estimation	Two-planes	Acquisition time	Noise-resolutiontrade off
	Multiple-planes	Higher resolution	More number of measurements

2.4 Refractive index variation based TIE

The monochromatic beam propagating along the z-axis passes through an object and tuneable refractive index medium with a thickness L. Under the paraxial approximation, the complex field $u(x,y,z)$ after passing the object,

$$u(x,y,z) = u_0(x,y,z)\, e^{-i\varphi(x,y)} \tag{12}$$

where $u_0(x,y,z)$ is the amplitude and $\varphi(x,y)$ carries the phase information of the object. After solving the propagation with angular spectrum method and taking derivative with n (refractive index of the medium), we obtain the differential equation as,

$$\frac{\partial u(x,y)}{\partial n} = \frac{iL}{2k_0 n^2}\nabla^2 u(x,y) - ik_0 L u(x,y) \tag{13}$$

It can be seen that Eq (13) is similar to the paraxial wave equation. So, TIE like equation can be derived to show the intensity-phase relation with the variation of refractive index in the medium. The modified TIE equation is [32,33],

$$\frac{\partial I(x,y,n)}{\partial n} = \frac{L}{k_0 n^2}\nabla\cdot(I\,\nabla\varphi) \tag{14}$$

Eqation (14) shows that phase information can be retrieved if the intensity variation is calculated with respect to the change in the refractive index.

3 Experimental results

The schematic diagram of the experimental set-up for TIE phase imaging based on refractive index variation is shown in Fig 1. A light emitting diode (LED) (central wavelength 630 nm, FWHM 13.1 nm) source has been used as illumination beam. A lens (focal length 75 mm) has been used for collimation of beam. The collimated beam is incident on the sample. Microscopic objective lens has been used to magnify the micro-sample. Two lenses (focal length 100 mm) of equal focal lengths have been used to make the 4*f* imaging setup to relay the image plane onto the CCD camera (make: The imaging source, 2592 × 1944 pixels, pixel size 22 µm). Before CCD, the liquid crystal variable retarder (make: Thorlabs) has been placed to vary the refractive index of the medium. The two images have been recorded at two refractive indices by a CCD

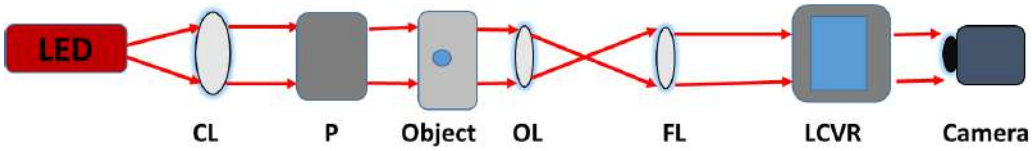

Fig1. Schematic diagram of the experimental set-up. LED: Light emitting diode, CL: Collimating lens, P: Polarizer, OL and FL: 4f imaging system, LCVR: Liquid crystal variable retarder [Ref 32]

camera, which are stored in computer. Then, the TIE has been solved in computer using MATLAB. The FFT-based Possion solver has been used to retrieve the phase map of the sample. Figures 2(a) and 3(a) represent the in-focus images of the USAF resolution chart and micro-lens array, respectively and Figs 2(b) and 3(b) show their retrieved phase maps.

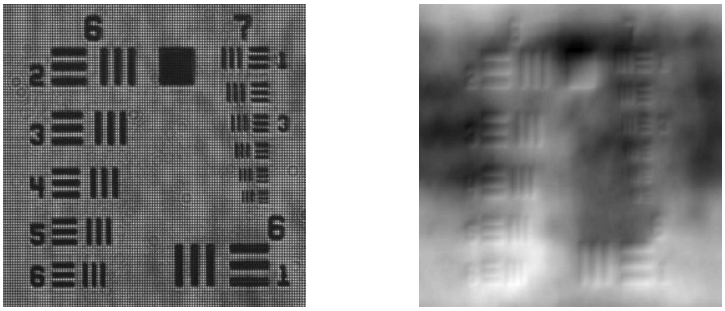

(a) (b)

Fig 2(a). In-focus intensity image of USAF resolution chart and (b) retrieved phase map [Ref. 33]

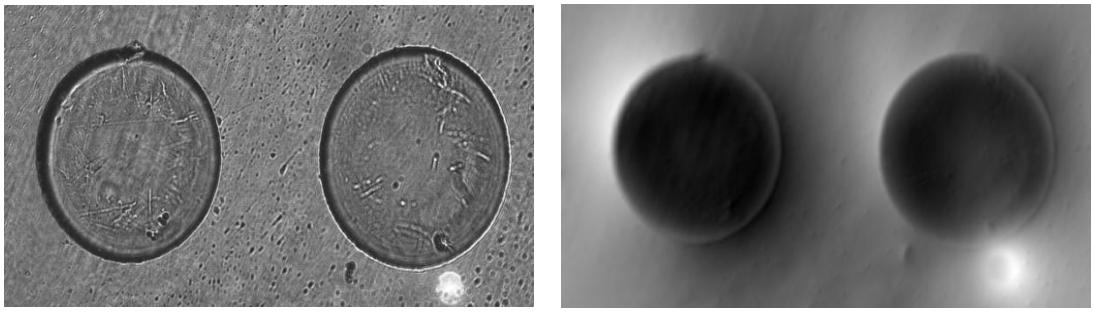

(a) (b)

Fig 3(a). In-focus intensity image of micro-lens array and (b) retrieved phase map

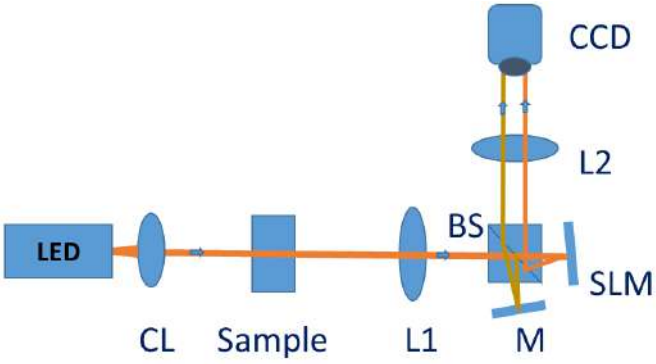

Fig 4. Schematic diagram of the experimental set-up. LED: Light emitting diode, CL: collimating lens, L1 and L2: 4*f* imaging system, M: Mirror, SLM: Spatial light modulator, CCD: Charge-coupled device [Ref 42].

The set-up for single shot experiment based on SLM is shown in Fig 4. Similar to previous experiment, the two lenses of equal focal lengths have been used to make the 4*f* imaging setup to relay the

image plane onto the CCD. In between two lenses of 4 *f* imaging, a mirror and a liquid crystal SLM (PLUTO, make: Holoeye) has been placed. The mirror and the SLM have been given a small tilt to avoid overlapping such that the two images have been recorded in one single-shot image.

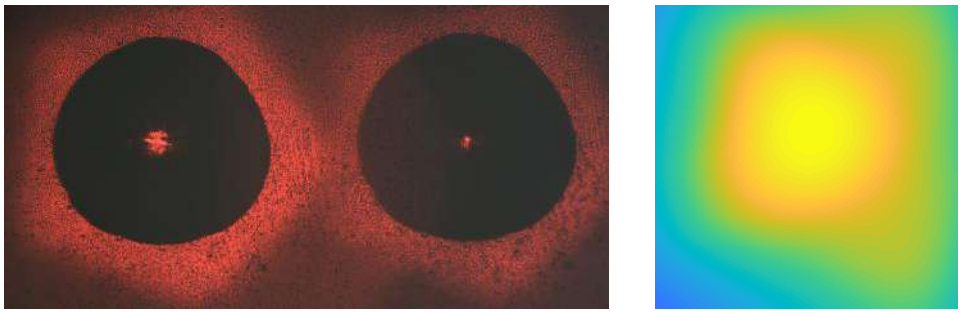

(a) (b)

Fig 5(a) Single-shot intensity image of glue-dropand (b) Retrieved phase map [Ref 42]

The single-shot image has been recorded which carries two images at two refractive indices. The two images have been separated and similarly the TIE has been solved using MATLAB. The FFT based Possion solver has been used to retrieve the phase map of the sample. Figure 5(a) presents a single shot image of the ultra-violet glue-drop and Fig 5(b) shows its retrieved phase map.

4 Discrepancy due to Teague's assumption

As we know, the generalized solution of TIE is solved by assuming the Teague's auxiliary function [13]. It is considered that the transverse flux is conservative such that the scalar potential exists which satisfy the TIE. Allen *et al* [59] pointed out a problem with the auxiliary function that it doesn't always exist since the transverse energy flux may not be conservative, and consequently it would yield the results other than the exact solution. Schmalz *et al* [60] provided a detailed explanation based on the Helmholtz decomposition theorem and decomposed the transverse flux in terms of the gradient of a scalar potential ψ and the curl of a vector potential η:

$$I\nabla\varphi = \nabla\psi + \nabla\times\eta \tag{15}$$

It is clearly visible that the term $\nabla\times\eta$ is not considered in Teague's assumption, assuming silently that the transverse flux is not rotational. Zuo *et al* [61] solved this problem by taking the effect of the missing term on phase recovery. They derived the useful condition for the validity of Teague's assumption:

$$\nabla I^{-1}\times\nabla^{-2}[\nabla\cdot(\nabla I\times\nabla\varphi)] = 0 \tag{16}$$

The Eq (16) shows that if the in-focus intensity distribution is nearly uniform, the phase discrepancy resulting from the Teague's assumption is quite small. However, if the measured intensity distribution exhibits strong absorption, the phase discrepancy might be large and cannot be ignored [62]. Zuo *et al* [61] further developed a simple Picard-type iterative algorithm to compensate the phase discrepancy due to Teague's assumption, in which within a few iterations, the phase discrepancy can be reduced to a very minimal level, which leads to the exact solution to the TIE.

5 Conclusions

The TIE is propagation based non-interferometric phase imaging method, in which we let the phase contrast be formed after slight defocus from the image plane. The TIE is valid under the paraxial approximation in the near Fresnel region (small defocusing separation). TIE is simply based on propagated intensity distribution along the optic axis, which needs two or more intensity distributions. The absolute phase map

can be directly recovered without need of phase unwrapping process. A modification in TIE has also been discussed where intensity stack has been recorded at different refractive indices. Any phase shifter device can be utilized for refractive index variation. Most important thing is that TIE is valid even in the partial coherence illumination.

Acknowledgment

Mr Rouchin Mahendra from IRDE Dehradun, India is acknowledged for providing micro-lens array.

References

1. Zernike F, How I discovered phase contrast, *Science*, 121(1955)345-349.
2. Nomarski G, Differential microinterferometer with polarized waves, *J Phys Radium*, 16(1955)9S-13S.
3. Bernet S, Jesacher A, Furhapter S, Maurer C, Ritsch-Marte M, Quantitative imaging of complex samples by spiral phase contrast microscopy, *Opt Express*, 14(2006)3792-3805.
4. Nehmetallah G, Banerjee P P, Applications of digital and analog holography in 3D imaging, *Adv Opt Photonics*, 4(2012)472-553.
5. Schnars U, Falldorf C, Watson J, Jüptner W, Digital Holography and Wavefront Sensing, (Springer), 2014.
6. Kim M K, Principles and techniques of digital holographic microscopy, *SPIE Rev*, 1(2010)018005; doi. 10.1117 /6.0000006.
7. Charrière F, Kühn J, Colomb T, Montfort F, Cuche E, Emery Y, Weible K, Marquet P, Depeursinge C, Characterization of microlenses by digital holographic microscopy, *Appl Opt*, 45(2006)829-835.
8. Kemper B, Bally G V, Digital holographic microscopy for live cell applications and technical inspection, *Appl Opt*, 47(2008)A52-A61; doi.org/10.1364/AO.47.000A52
9. Marquet P, Rappaz B, Magistretti P J, Cuche E, Emery Y, Colomb T, and Depeursinge C, Digital holographic microscopy: a noninvasive contrast imaging technique allowing quantitative visualization of living cells with subwavelength axial accuracy, *Opt Lett*, 30(2005)468-470.
10. Maiden A M, Rodenburg J M, Humphry M J, Optical ptychography: a practical implementation with useful resolution, *Opt Lett*, 35(2010)2585-2587.
11. Marrison J, Raty L, Marriot P, O'Toole P, Ptychography – a label free, high-contrast imaging technique for live cells using quantitative phase information, *Sci Rep*, 3(2013)2369; doi.org/10.1038/srep02369
12. Ou X, Horstmeyer R, Yang C, Zheng G, Quantitative phase imaging via Fourier ptychographic microscopy, *Opt Lett*, 38(2013)4845-4848.
13. Teague M R, Deterministic phase retrieval: A Green's function solution, *J Opt Soc Am*, 73(1983)1434-1441.
14. Streibl N, Phase imaging by the transport equation of intensity, *Opt Commun*, 49(1984)6-10.
15. Paganin D, Nugent KA, Non-interferometric phase imaging with partially coherent light, *Phys Rev Lett*, 80(1998)2586-2589.
16. Roddier F, Roddier C, Roddier N, Curvature sensing: A new wavefront sensing method, *Procd 32nd Annual International Tech. Sym. on Optical and Optoelectronic Applied Science and Engineering*, San Diego, CA, USA, (1988).
17. Ishizuka A, Mitsuishi K, Ishizuka K, Direct observation of curvature of the wave surface in transmission electron microscope using transport intensity equation, *Ultramicroscopy*, 194(2018)7-14.
18. Bajt S, Barty A, Nugent K, McCartney M, Wall M, Paganin D, Quantitative phase-sensitive imaging in a transmission electron microscope, *Ultramicroscopy*, 83(2000)67-73.
19. Ishizuka A, Ishizuka K, Mitsuishi K, Boundary-artifact-free observation of magnetic materials using the transport of intensity equation, *Microsc Microanal*, 24(2018)924-925.
20. Nugent K A, Coherent methods in the X-ray sciences, *Adv Phys*, 59 (2010)1-99.
21. Schmalz J A, Gureyev T E, Paganin D M, Pavlov K M, Phase retrieval using radiation and matter-wave fields: Validity of Teague's method for solution of the transport-of-intensity equation, *Phys Rev A*, 84(2011)023808; doi. org/10.1103/PhysRevA.84.023808.

22. Allman B, McMahon P, Nugent K, Paganin D, Jacobson D, Arif M, Werner S, Phase radiography with neutrons, *Nature*, 408(2000)158-159.
23. Chen N, Zuo C, Lam E Y, Lee B, 3D Imaging based on depth measurement technologies, *Sensors*, 18(2018)3711; doi.org/10.3390/s18113711.
24. Komuro K, Yamazaki Y, Nomura T, Transport of intensity computational ghost imaging, *Appl Opt*, 57(2018)4451-4456.
25. Barty A, Nugent K, Paganin D, Roberts A, Quantitative optical phase microscopy, *Opt Lett*, 23(1998)817-819.
26. Zuo C, Chen Q, Qu W, Asundi A, High-speed transport-of-intensity phase microscopy with an electrically tunable lens, *Opt Express*, 21(2013)24060-24075.
27. Waller L, Luo Y A, Yang S Y, Barbastathis G, Transport of intensity phase imaging in a volume holographic microscope, *Opt Lett*, 35(2010)2961-2963.
28. Waller L, Kou S S, Sheppard C J R, Barbastathis G, Phase from chromatic aberrations, *Opt Express*, 18(2010) 22817-22825.
29. Camacho L, Mico V, Zalevsky Z, Garcia J, Quantitative phase microscopy using defocusing by means of a spatial light modulator, *Opt Express*, 18(2010)6755-6766.
30. Agour M, Falldorf C, Kopylow C, Bergmann R B, Automated compensation of misalignment in phase retrieval based on a spatial light modulator, *Appl Opt*, 50(2011)4779-4787.
31. Gorthi S S, Schonbrun E, Phase imaging flow cytometry using a focus-stack collecting microscope, *Opt Lett*, 37(2012)707-709.
32. Chen C-H, Hsu H-F, Chen H-R, Hsieh W-F, Non-interferometric phase retrieval using refractive index manipulation, *Sci Rep*, 7(2017)46223; doi: 10.1038/srep46223 (2017).
33. Gupta A K, Fatima A, Nishchal N K, Phase imaging based on transport of intensity equation using liquid crystal variable waveplate, in *Digital Holography and Three-Dimensional Imaging 2019*, OSA Tech. Digest (2019), paper M5B.4.
34. Gupta A K, Nishchal N K, Phase retrieval using liquid crystal variable retarder based on reference-less non-interferometric technique, *Optical Society of India - International Symposium on Optics 2018*, Kanpur, India.
35. Gupta A K, Nishchal N K, A non-interferometric phase retrieval using liquid crystal spatial light modulator, *The Int'l. Confer. on Fiber Optics and Photonics* (PHOTONICS-2018), Dec. 12-15, 2018, IIT Delhi.
36. Paganin D, Mayo S C, Gureyev T E, Miller P R, Wilkins S W, Simultaneous phase and amplitude extraction from a single defocused image of a homogeneous object, *J Microsc*, 206(2002)33-40.
37. Poola P K, John R, Label-free nanoscale characterization of red blood cell structure and dynamics using single-shot transport of intensity equation, *J Biomed Opt*, 22(2017)106001; doi.org/10.1117/1.JBO.22.10.106001
38. Zuo C, Chen Q, Qu W, Asundi A, Noninterferometric single-shot quantitative phase microscopy, *Opt Lett*, 38(2013)3538-3541.
39. Nguyen T, Nehmetallah G, Non-interferometric tomography of phase objects using spatial light modulators, *J Imaging,* **2**(2016)1-16.
40. Yu W, Tian X, He X, Song X, Xue L, Liu C, Wang S, Real time quantitative phase microscopy based on single-shot transport of intensity equation method, *Appl Phys Lett*, 109(2016)071112; doi.org/10.1063/1.4961383.
41. Zhou W-J, Guan X, Liu F, Yu Y, Zhang H, Poon T-C, Banerjee P P, Phase retrieval based on transport of intensity and digital holography, *Appl Opt*, 57(2018) A229-A234.
42. Gupta A K, Nishchal N K, Single-shot transport of intensity equation based phase imaging using refractive index variation, *Digital Holography and Three-Dimensional Imaging*, OSA Tech. Digest 2019, paper M5B.7.
43. Woods S C, Greenaway A H, Wavefront sensing by use of a Green's function solution to the intensity transport equation, *J Opt Soc Am A*, 20(2003)508-512.
44. Pinhasi S V, Alimi R, Perelmutter L, Eliezer S, Topography retrieval using different solutions of the transport intensity equation, *J Opt Soc Am A*, 27(2010)2285-2292.
45. Gureyev T E, Roberts A, Nugent K A, Phase retrieval with the transport-of-intensity equation: Matrix solution with use of Zernike polynomials, *J Opt Soc Am A*, 12(1995)1932-1941.

46. Gureyev T E, Nugent K A, Phase retrieval with the transport-of-intensity equation. II. Orthogonal series solution for nonuniform illumination, *J Opt Soc Am A,* 13(1996)1670-1682.
47. Huang L, Zuo C, Idir M, Qu W, Asundi A, Phase retrieval with the transport-of-intensity equation in an arbitrarily shaped aperture by iterative discrete cosine transforms, *Opt Lett*, 40(2015)1976-1979.
48. Volkov V, Zhu Y, Graef M D, A new symmetrized solution for phase retrieval using the transport of intensity equation, *Micron,* 33(2002)411-416.
49. Frank J, Altmeyer S, Wernicke G, Non-interferometric, non-iterative phase retrieval by Green's functions, *J Opt Soc Am A*, 27(2010)2244-2251.
50. Zuo C, Chen Q, Asundi A, Boundary-artifact-free phase retrieval with the transport of intensity equation: Fast solution with use of discrete cosine transform, *Opt Express*, 22(2014)9220-9244.
51. Martinez-Carranza J, Falaggis K, Kozacki T, Kujawinska M, "Effect of imposed boundary conditions on the accuracy of the transport of intensity equation based solvers, *Proc SPIE* 8789, 87890N (2013); doi.org/10.1117/12.2020662
52. Paganin D, Barty A, McMahon P J, Nugent K A, Quantitative phase-amplitude microscopy. III. The effects of noise, *J Microsc*, 214(2004)51-61.
53. Zuo C, Chen Q, Yu Y, Asundi A, Transport-of-intensity phase imaging using Savitzky-Golay differentiation filter-theory and applications, *Opt Express*, 21(2013)5346-5362.
54. Cong W, Wang G, Higher-order phase shift reconstruction approach: Higher-order phase shift reconstruction approach, *Med Phys*, 37(2010)5238-5242.
55. Waller L, Tian L, Barbastathis G, Transport of intensity phase-amplitude imaging with higher order intensity derivatives, *Opt Express*, 18(2010)12552-12561.
56. Bie R, Yuan X H, Zhao M, Zhang L, Method for estimating the axial intensity derivative in the TIE with higher order intensity derivatives and noise suppression, *Opt Express*, 20(2012)8186-8191.
57. Soto M, Acosta E, Improved phase imaging from intensity measurements in multiple planes, *Appl Opt*, 46(2007) 7978-7981.
58. Medhi B, Hegde G M, Reddy K J, Roy D, Vasu R M, Shock-wave imaging by density recovery from intensity measurements, *Appl Opt*, 57(2018)4297-4308.
59. Allen L, Oxley M, Phase retrieval from series of images obtained by defocus variation, *Opt Commun*, 199(2001) 65-75.
60. Schmalz J A, Gureyev T E, Paganin D M, Pavlov K M, Phase retrieval using radiation and matter-wave fields: Validity of Teague's method for solution of the transport-of-intensity equation, *Phys Rev A*, 84(2011)023808; doi. org/10.1103/PhysRevA.84.023808
61. Zuo C, Chen Q, Huang L, Asundi A, Phase discrepancy analysis and compensation for fast Fourier transform based solution of the transport of intensity equation, *Opt Express*, 22(2014)17172-17186.
62. Ferrari J A, Ayubi G A, Flores J L, Perciante C D, Transport of intensity equation: Validity limits of the usually accepted solution, *Opt Commun*, 318(2014)133-136.

[Received: 27.08.2019; *revised recd* :12.09.2019; *accepted* : 23.09.2019]